



Pacific Northwest
NATIONAL LABORATORY

Proudly Operated by Battelle Since 1965

Field measurement of velocity time series in the center of Sequim Bay

October 2017

SF Harding

GEL Harker-Klimeš

DISCLAIMER

This report was prepared as an account of work sponsored by an agency of the United States Government. Neither the United States Government nor any agency thereof, nor Battelle Memorial Institute, nor any of their employees, makes **any warranty, express or implied, or assumes any legal liability or responsibility for the accuracy, completeness, or usefulness of any information, apparatus, product, or process disclosed, or represents that its use would not infringe privately owned rights.** Reference herein to any specific commercial product, process, or service by trade name, trademark, manufacturer, or otherwise does not necessarily constitute or imply its endorsement, recommendation, or favoring by the United States Government or any agency thereof, or Battelle Memorial Institute. The views and opinions of authors expressed herein do not necessarily state or reflect those of the United States Government or any agency thereof.

PACIFIC NORTHWEST NATIONAL LABORATORY

operated by

BATTELLE

for the

UNITED STATES DEPARTMENT OF ENERGY

under Contract DE-AC05-76RL01830

Printed in the United States of America

Available to DOE and DOE contractors from the
Office of Scientific and Technical Information,
P.O. Box 62, Oak Ridge, TN 37831-0062;
ph: (865) 576-8401
fax: (865) 576-5728
email: reports@adonis.osti.gov

Available to the public from the National Technical Information Service,
U.S. Department of Commerce, 5285 Port Royal Rd., Springfield, VA 22161
ph: (800) 553-6847
fax: (703) 605-6900
email: orders@ntis.fedworld.gov
online ordering: <http://www.ntis.gov/ordering.htm>



This document was printed on recycled paper.

(9/2003)

Field measurement of velocity time series in the center of Sequim Bay

SF Harding

G Harker-Klimes

October 2017

Prepared for
the U.S. Department of Energy
under Contract DE-AC05-76RL01830

Pacific Northwest National Laboratory
Richland, Washington 99352

Summary

A 600 kHz RDI Workhorse was installed in the center of Sequim Bay from 15:04 June 23, 2017 to 09:34 August 24, 2017 at a depth of 25.9 m below MLLW. The instrument was configured to record the flow velocity in vertical cells of 1.0 m in 10 minute ensembles. Each ensemble was calculated as the mean of 24 pings, sampled with an interval of 5.0 s. A burst of increased sampling rate (1200 samples at 2 Hz) was recorded to characterize the wave climate on an hourly basis.

The peak depth-averaged flow speed for the deployment was recorded during the flood tide on June 24, 2017 with a magnitude of 0.34 m/s. The peak flow speed in a single bin was recorded during the same tide at a location of 11.6 m from the seabed with a magnitude of 0.46 m/s. Significant flow speeds were only observed in the flood tides, while the ebb tide flow speeds were negligible throughout the deployment. The velocity direction was observed to be relatively constant as a function of depth during flood tides but highly variable during times of slower ebb tides.

A peak significant wave height of 0.36 m was recorded on June 30, 2017 at 18:54. The measured waves showed no indication of a prevalent wave direction during this deployment. The wave record of the fetch-limited site during this deployment approaches the lower limit of the wave measurement resolution.

The water temperature fluctuated over a range of 1.7°C during the deployment duration. The mean pitch of the instrument was -1.2° and the mean roll angle of the instrument was 0.3°. The low pitch and roll angles are important factors in the accurate measurement of the wave activity at the surface.

Acknowledgments

The authors wish to thank Sue Southard for operational guidance and health and safety overview, John Vavrinec, Kate Hall and Garrett Staines for assistance with vessel operations during deployment and retrieval, and Shon Zimmerman for providing the illustration of depth contours in the region of Sequim Bay inlet.

Acronyms and Abbreviations

ADCP	Acoustic Doppler current profiler
FAU	Florida Atlantic University
MLLW	Mean Lower Low Water
MSL	Marine Sciences Laboratory of PNNL
PNNL	Pacific Northwest National Laboratory

Contents

Summary	iii
Acknowledgments.....	v
Acronyms and Abbreviations	vii
1.0 Introduction	1
2.0 Method.....	1
2.1 Deployment overview	1
2.2 Instrument deployment.....	3
2.3 Instrument retrieval	5
3.0 Data processing.....	5
4.0 Results	6
5.0 References	18
Appendix A – ADCP Operating Principle.....	A.1
Appendix B – Deployment configuration file.....	B.1
Appendix C – Contour plots of velocity direction.....	C.1

Figures

Figure 1: Location of ADCP deployment, showing depth contours of Sequim Bay Inlet.....	2
Figure 2: ADCP in Sea Spider mount showing acoustic release, retrieval buoy, lead ballast and plywood feet.	3
Figure 3: Zinc oxide paste on ADCP transducers.....	4
Figure 4: Biofouling on ADCP and Sea Spider at time of retrieval.....	5
Figure 5: Contour plot of velocity magnitude (m/s) in June, 2017. The water depth at the ADCP location is indicated with a white line.	7
Figure 6: Contour plot of velocity magnitude (m/s) in July, 2017. The water depth at the ADCP location is indicated with a white line.	8
Figure 7: Contour plot of velocity magnitude (m/s) in August, 2017. The water depth at the ADCP location is indicated with a white line.....	9
Figure 8: Depth-averaged velocity magnitude in June, 2017	10
Figure 9: Depth-averaged velocity magnitude in July, 2017	11
Figure 10: Depth-averaged velocity magnitude in August, 2017	12
Figure 11: Daily maximum velocity magnitude during deployment	13
Figure 12: Contour plot of velocity magnitude and direction of peak flow speed during deployment.	13
Figure 13: Water depth (top), depth-averaged velocity magnitude (middle) and depth-average flow direction (bottom) for tide of peak flow speed during deployment	14
Figure 14: Scatter plot of velocity using velocities from the depth of the fastest velocity recording (left) and depth-averaged velocities (right).....	15
Figure 15: Water level time series from ADCP measurements and NOAA high/low tidal elevation prediction.	15
Figure 16: Comparison of NOAA tidal elevation prediction and ADCP measurements.....	16
Figure 17: Distribution of significant wave height during deployment	16
Figure 18: Ancillary data of instrument pitch, roll and heading (top) and water temperature (bottom) throughout the deployment.	17
Figure 19: Schematic of RDI Workhorse Sentinel ADCP (left), showing the direction of the transmitted acoustic signal in grey, and the reflected signal in black. Beam velocity schematic (right) shows how a velocity vector is projected as a beam-wise component and a cross-beam component. Cardinal directions given in the right-side figure are for descriptive purposes only (RDI, 1996).	A.2

Tables

Table 1: 600 kHz ADCP deployment parameters.....	3
--	---

1.0 Introduction

An Acoustic Doppler Current Profiler (ADCP) was installed in the middle of Sequim Bay Inlet for 63 days as part of the Triton Initiative, in support of two project awards from the US Department of Energy: Integral Consulting Inc, and Florida Atlantic University (FAU). This characterizes the conditions during the Integral and FAU deployments, while also increasing the understanding of the flow velocity magnitudes and time series within the deeper parts of Sequim Bay.

This report presents the results of this ADCP deployment.

2.0 Method

2.1 Deployment overview

An ADCP was deployed in Sequim Bay Inlet for 63 days from June 23 to August 24, 2017. This instrument was used to measure flow velocity, water depth, and wave climate during this time. The ADCP was deployed at 48° 3.4900' N, 123° 1.4560' W at a depth of 25.9 m below MLLW, as shown in Figure 1. The operating principles of the ADCP are summarized in Appendix A.

The ADCP selected for this survey was the RD Instruments 600 kHz Workhorse. This was mounted on a Teledyne Oceanscience Sea Spider tripod base, shown in Figure 2.

The seabed at the deployment site in the middle of Sequim Bay was known to be soft mud with fine sediments. As such, excessive ballast would likely cause the Sea Spider to sink into the mud, making retrieval difficult and risk obscuring the transducers of the ADCP. The ballast used on this deployment was 15 lb. of lead weight on each of the three feet. The submerged weight of the fiber-glass Sea Spider frame is approximately 50 lb. A 10" diameter buoy was attached to an acoustic release (InterOcean Systems, Inc., Model 111) on the Sea Spider for ease of locating the instrument in case of low visibility during retrieval. This added approximately 20 lb. of buoyancy for a total submerged weight of 75 lb.

Plywood feet measuring 300 mm x 300 mm were also added to the Sea Spider to distribute the weight of the deployment over a larger area in an effort to avoid sinking into the mud. These were fastened to the Sea Spider legs using cable ties for ease of removal by divers if the feet were not able to be extracted from the mud at the same time as the Sea Spider.

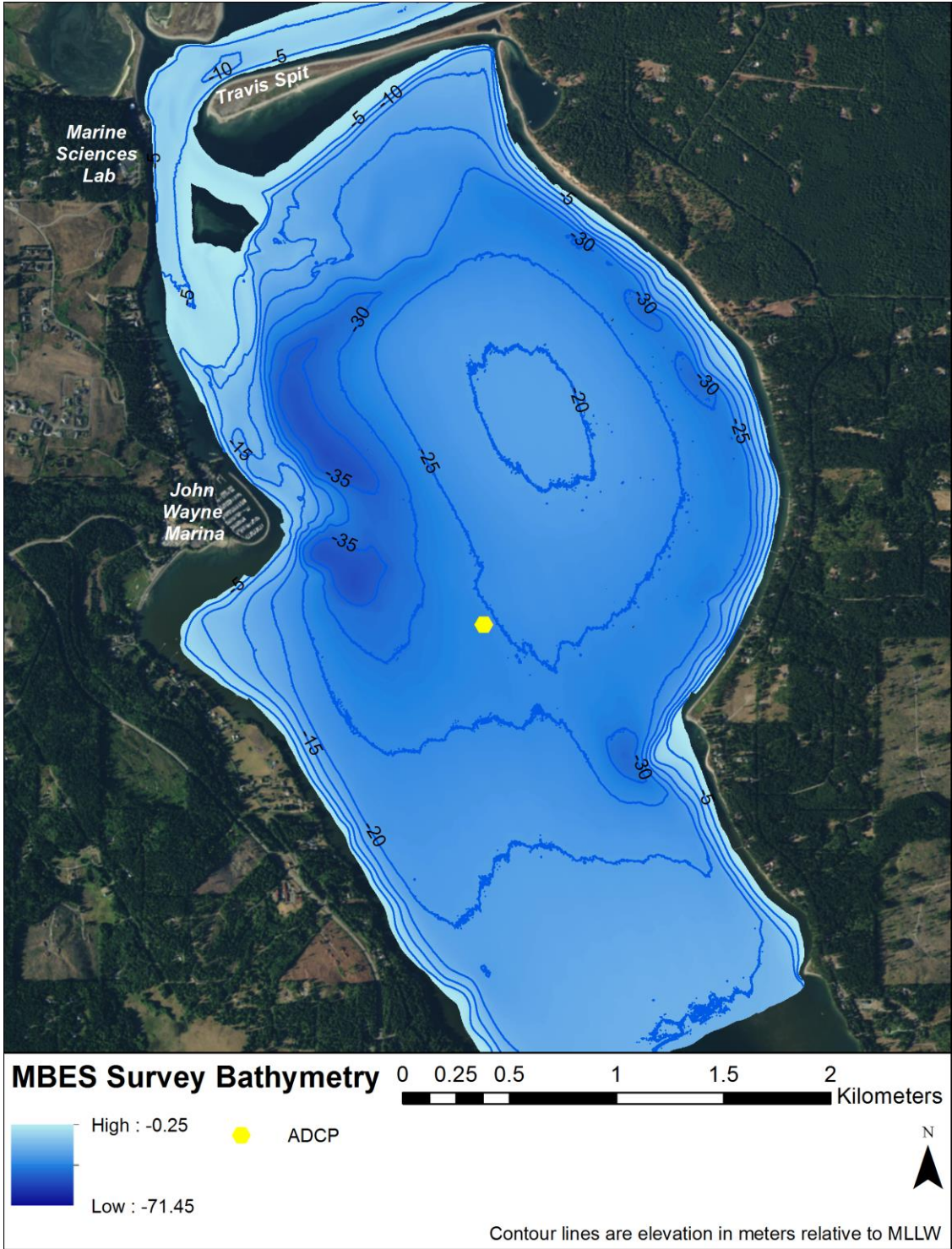


Figure 1: Location of ADCP deployment, showing depth contours of Sequim Bay Inlet



Figure 2: ADCP in Sea Spider mount showing acoustic release, retrieval buoy, lead ballast and plywood feet.

2.2 Instrument deployment

The profiling parameters used for this deployment are summarized in Table 1.

Table 1: 600 kHz ADCP deployment parameters

Parameter	Value
Blanking distance	0.88 m
Bin size	1.00 m
Number of bins	35
Sampling (ping) frequency	2 Hz
Water measurement pings/ensemble	24
Standard error of velocity ensemble	0.014 m/s

Ensemble averaging was used to calculate the mean velocity of 25 consecutive samples, to reduce the standard deviation from $\sigma_1 = 7.0$ cm/s (single sample) to $\sigma_N = 1.4$ cm/s.

The deployment configuration file is included in Appendix B.

The ADCP head was orientated such that the buoy was between two of the diverging acoustic beams to avoid acoustic signal interference. A zinc oxide paste was applied to the transducer head to minimize biofouling which can obscure the acoustic signal, as shown in Figure 3.

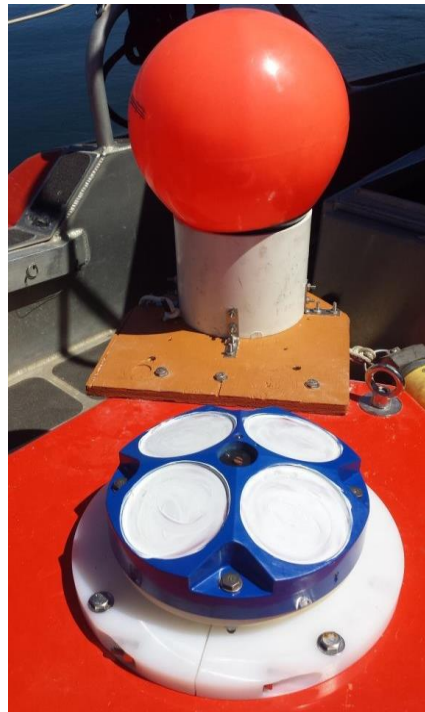


Figure 3: Zinc oxide paste on ADCP transducers

The Sea Spider was lowered to the seabed using the davit winch on the Desdemona research vessel (PNNL) and was deployed with a quick release clamp.

2.3 Instrument retrieval

Divers were used to retrieve the device, with audio communication to the boat crew. This process began with the acoustic release of the retrieval buoy to locate the instrument. Divers followed the line from the buoy to the Sea Spider and attached the shackle of the winch line to the lifting eye on the Sea Spider and then vacated the region.

The Sea Spider was submerged in the mud to the level of the “knee” of the tripod legs, below which very little biofouling was observed. The Sea Spider was retrieved with the plywood feet connected to the feet.

The retrieved ADCP is shown in Figure 4.



Figure 4: Biofouling on ADCP and Sea Spider at time of retrieval

3.0 Data processing

The beam-wise velocity vectors are combined to calculate a three-dimensional velocity vector, first in the instrument coordinate system and then in the earth coordinate system. These coordinate transforms are described in Appendix A.

The velocity profiles collected by the ADCP were filtered to only show signal returns from 2.0 m below the detected surface. The surface was identified in each beam as the depth cell with the peak amplitude return. The shallowest depth cell of all four beams was used as the surface location. The data from the two bins closest to the surface were ignored in this analysis as they are often biased by surface reflection effects. Wave data was processed using RDI WavesMon which uses the velocity data in the bins near the surface to calculate the wave metrics.

4.0 Results

The velocity magnitude as a function of depth and time is shown for the deployment duration in the contour plots of Figure 5 to Figure 7. The water depth, measured with an onboard pressure sensor, is shown with a white line. The fastest flow speeds are associated with the flood tide direction (when the water elevation in the bay is increasing).

The depth-averaged velocity magnitude for the deployment duration is shown in Figure 8 to Figure 10. The daily maximum depth-averaged velocity magnitude is shown in Figure 11.

The peak depth-averaged flow speed for the deployment was recorded during the flood tide on June 24, 2017 with a magnitude of 0.34 m/s. This tide corresponds to the largest low-to-high tidal elevation change of the deployment. The peak flow speed in a single bin was recorded during the same tide at a location of 11.6 m from the seabed with a magnitude of 0.46 m/s (Figure 12). The velocity direction (degrees clockwise from true north) was observed to be relatively constant as a function of depth for the higher flow velocities (flood tides) but highly variable during times of slower flow (ebb tides) as illustrated in Figure 12. The water depth, depth-averaged velocity magnitude and depth-averaged flow direction of the peak flow are shown in Figure 13.

The flow direction of the flood tide is predominantly in the easterly direction which may be a localized effect of the bathymetry shown in Figure 1. A scatter plot of the tidal direction for the duration of the deployment is shown in Figure 14. The velocity direction as a function of depth and time is shown for the deployment duration in Appendix C.

The high and low tide elevations predicted by NOAA (Sequim Bay Entrance, WA, Station ID: 9444555) were compared to those measured by ADCP. The reference elevation of the NOAA data was in MLLW. The distance of the ADCP from MLLW was calculated as the mean of the daily minimum pressure readings. This value was subtracted from the ADCP pressure data for comparison with the NOAA high/low tide elevation predictions as shown in Figure 15. The ADCP pressure data were interpolated at the times of the high and low tide predicted by the NOAA model and the elevations were compared in Figure 16. The mean elevation difference between the NOAA predictions and ADCP high/low elevations was equal to -0.04 m and the standard deviation of the difference is equal to 0.14 m.

The wave activity was below the lower limit of the ADCP wave measurement resolution for the majority of the deployment. The fetch limited site results in very low wave heights and wave periods. For completeness, the unfiltered distribution of significant wave heights (H_s) throughout the deployment is presented in Figure 17 showing a peak significant wave height of 0.36 m was recorded on June 30, 2017 at 18:54. This was recorded during a flood tide when the wave direction was coming from the SE direction. This peak wave height is likely the result of the wave-current interaction with a component of the flood current direction flowing in the opposite direction to the waves. The measured waves showed no indication of a prevalent wave direction during this deployment.

Ancillary data of the deployment is provided in Figure 18. The water temperature varied over a range of 1.7°C during the deployment. The mean pitch of the instrument was -1.2° and the mean roll angle of the instrument was 0.3° and the mean heading of Beam 3 was 012°. The low pitch and roll angles are important factors in the accurate measurement of the wave activity at the surface.

The instrument pitch, roll and heading altered by 4.0°, 3.5° and 1.0°, respectively, during the first day of installation as the gravity base bedded into the seabed. These angles then gradually drifted over a range of 0.7, 0.6° and 0.6°, respectively, for the remainder of the deployment.

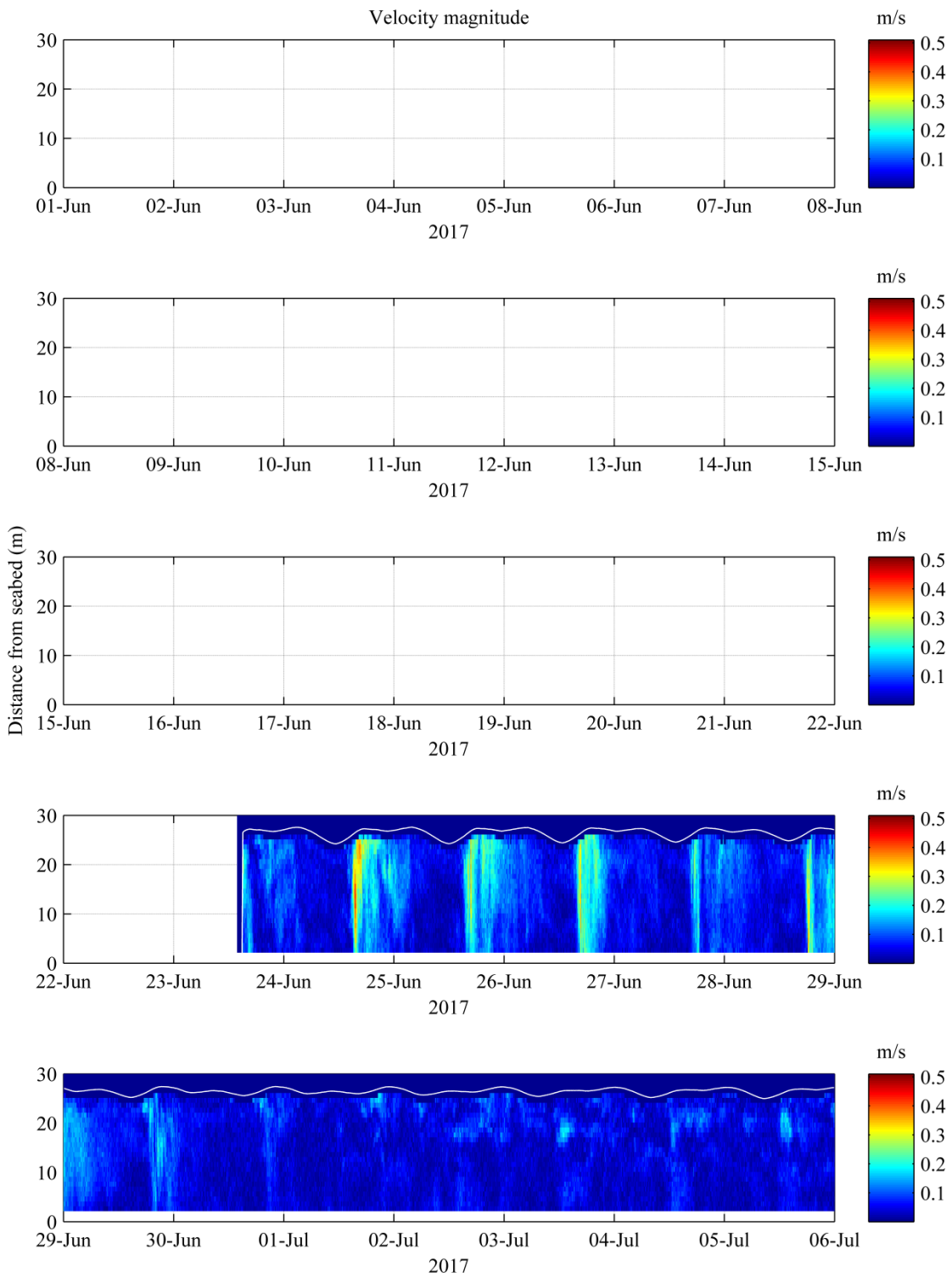


Figure 5: Contour plot of velocity magnitude (m/s) in June, 2017. The water depth at the ADCP location is indicated with a white line.

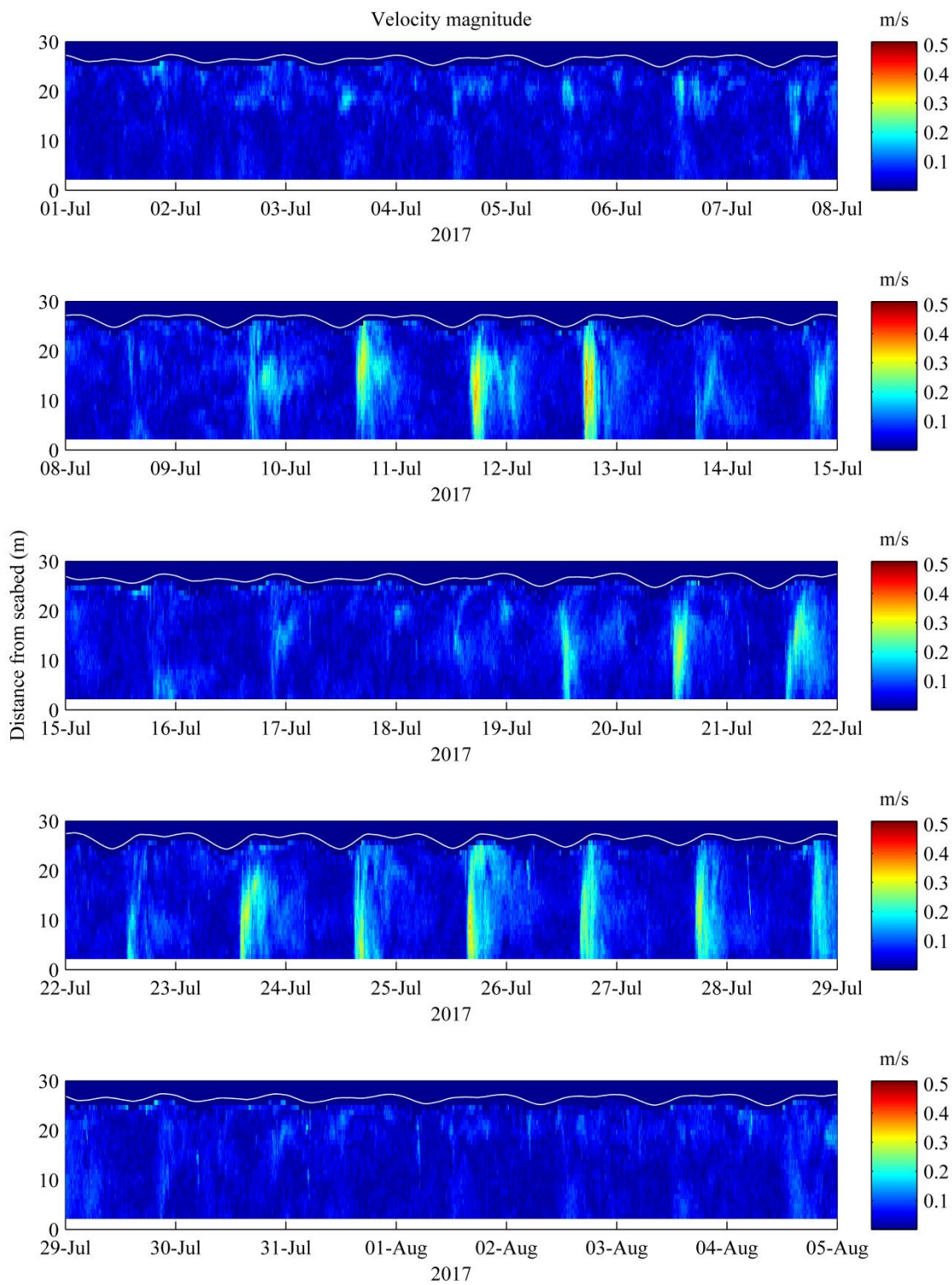


Figure 6: Contour plot of velocity magnitude (m/s) in July, 2017. The water depth at the ADCP location is indicated with a white line.

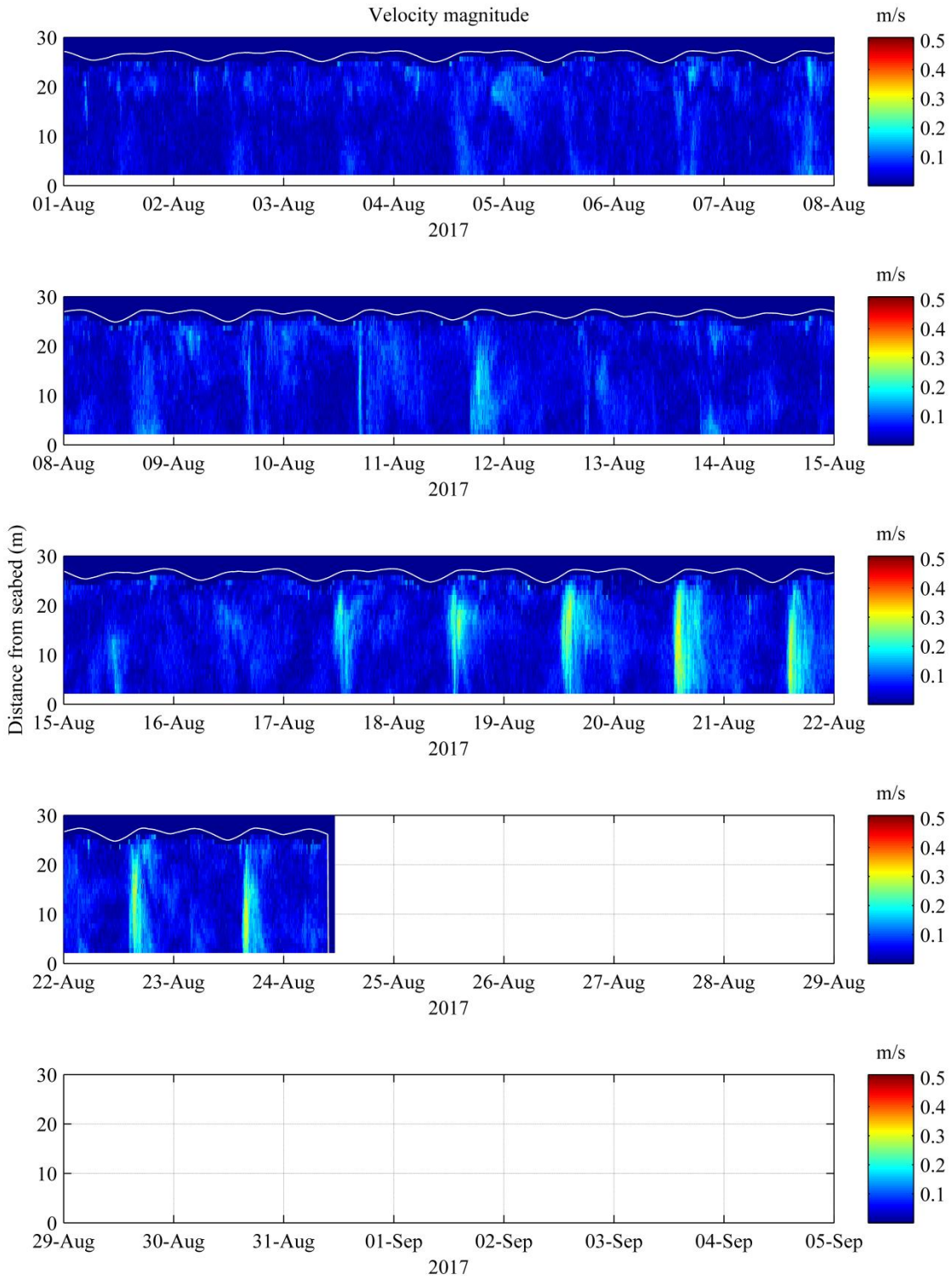


Figure 7: Contour plot of velocity magnitude (m/s) in August, 2017. The water depth at the ADCP location is indicated with a white line.

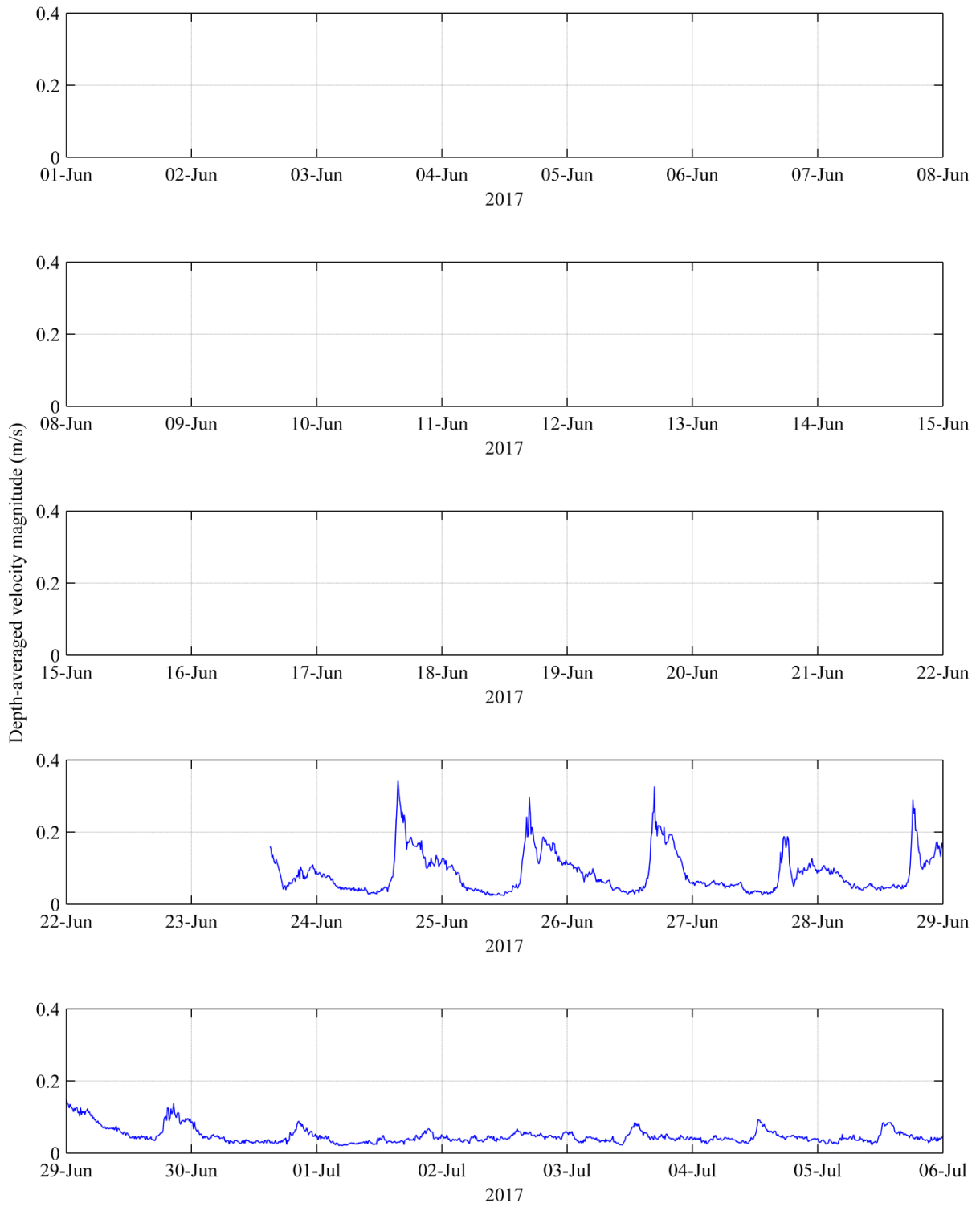


Figure 8: Depth-averaged velocity magnitude in June, 2017

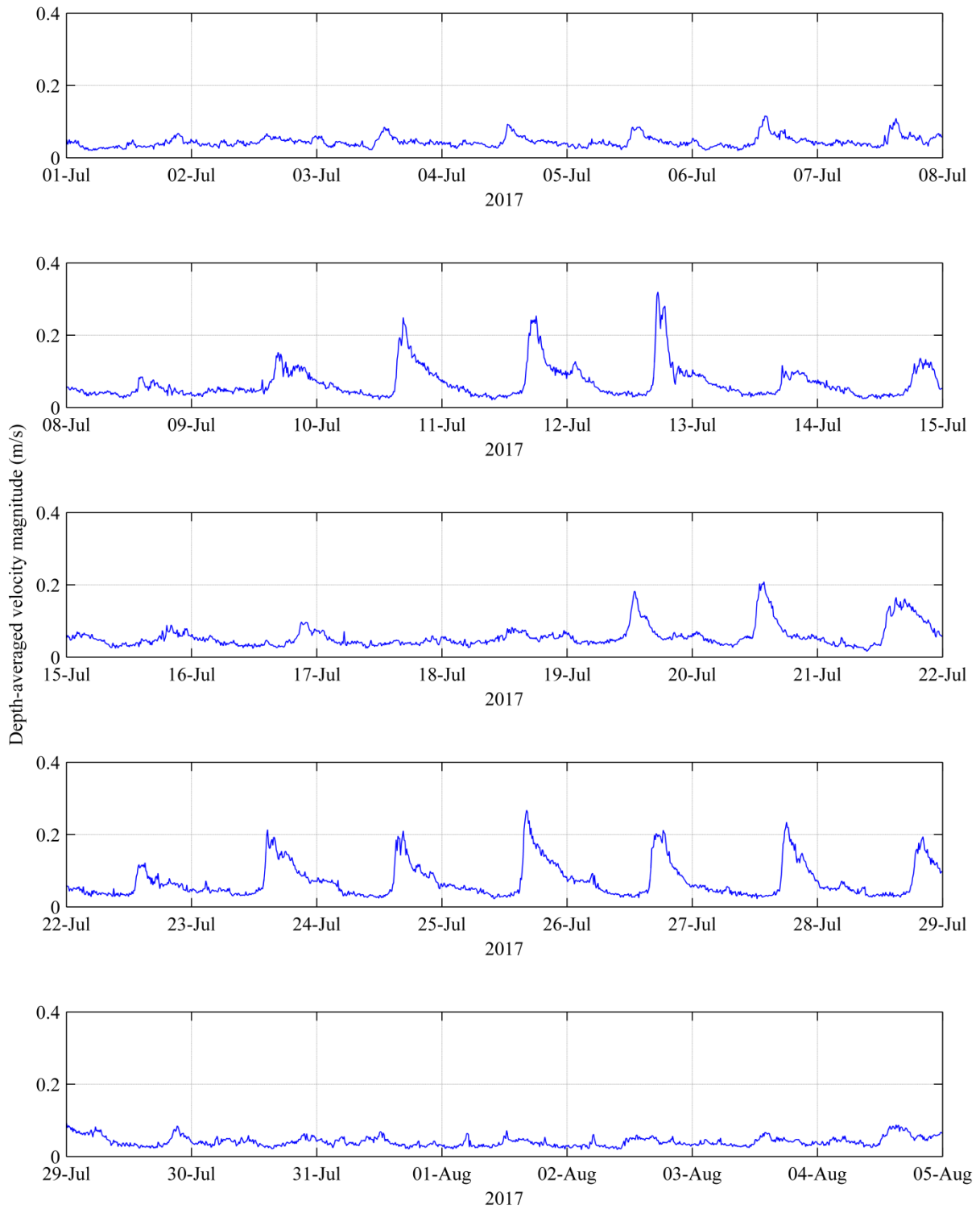


Figure 9: Depth-averaged velocity magnitude in July, 2017

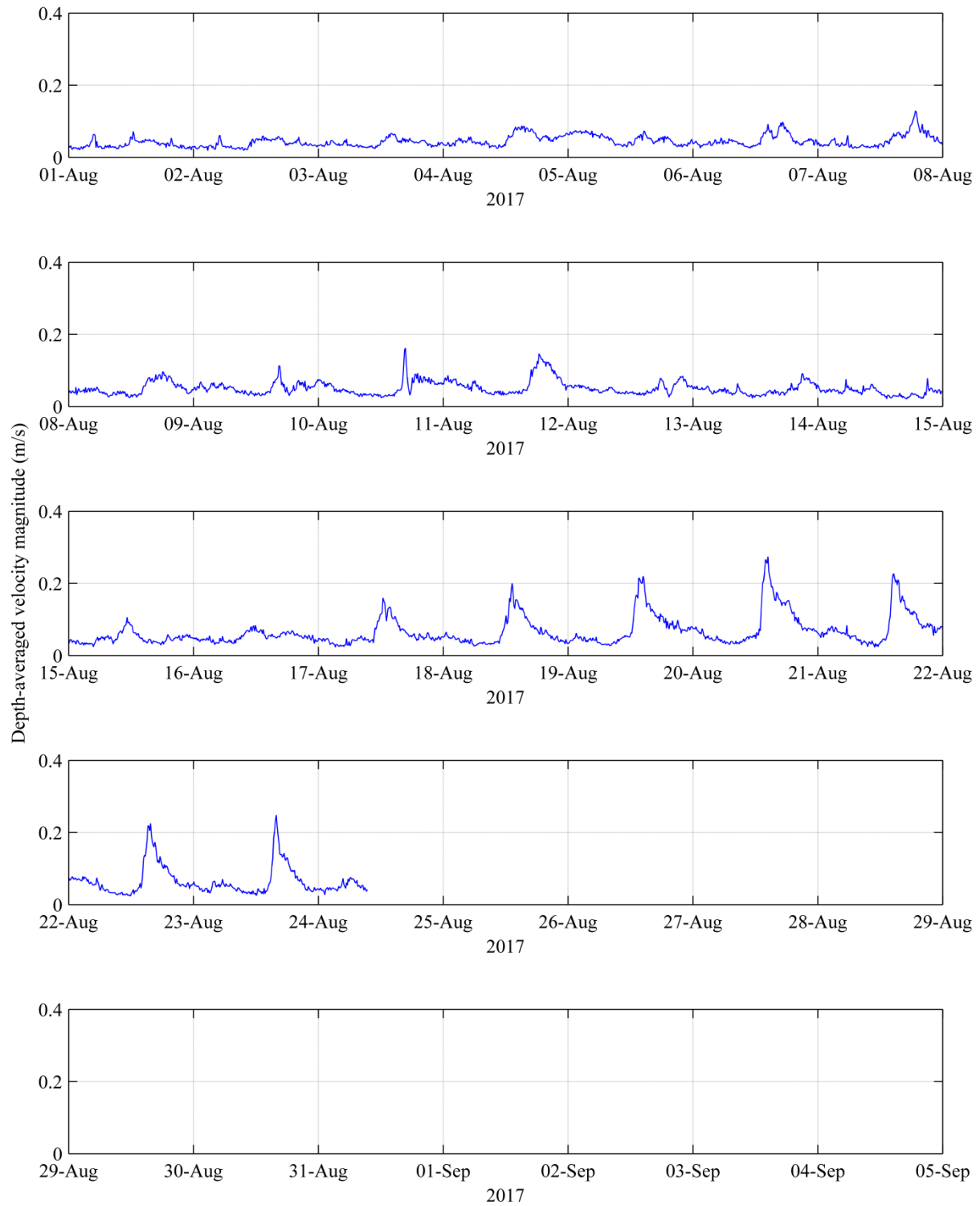


Figure 10: Depth-averaged velocity magnitude in August, 2017

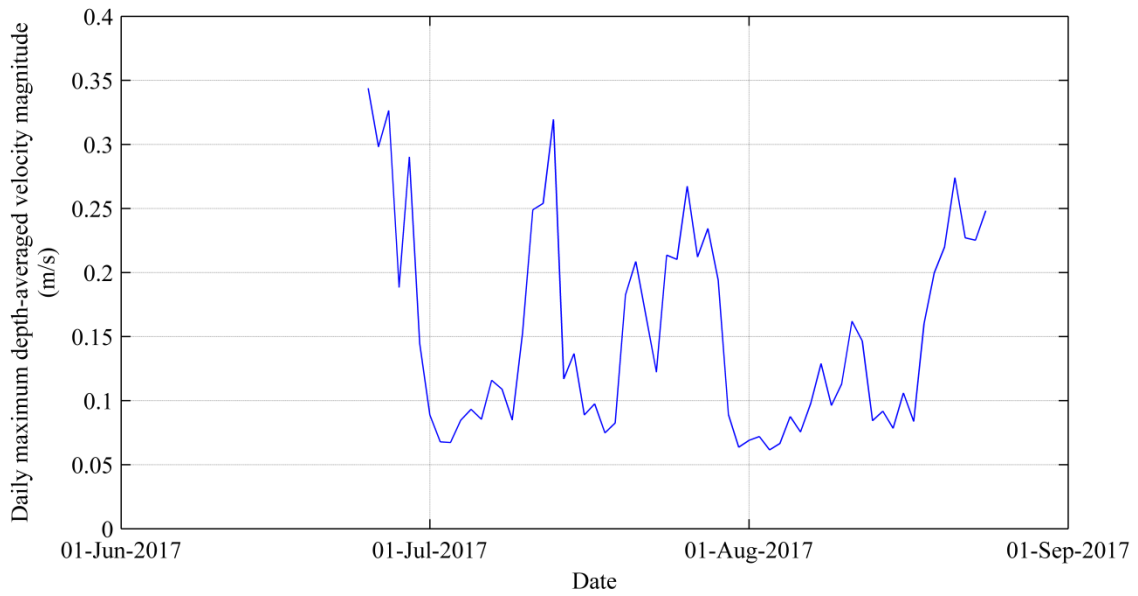


Figure 11: Daily maximum velocity magnitude during deployment

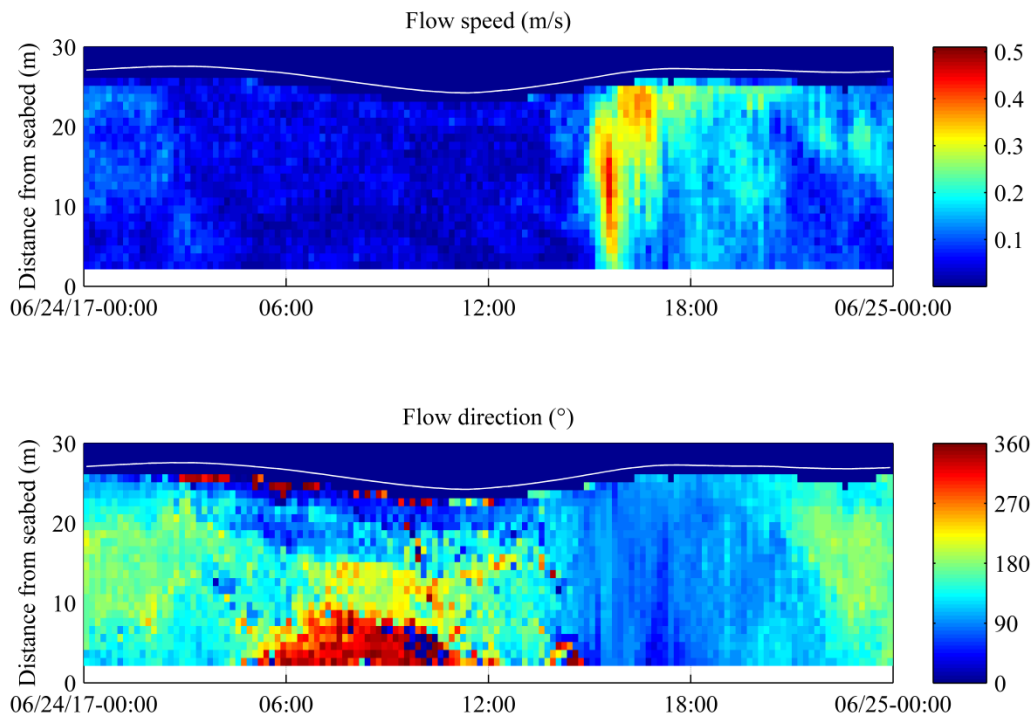


Figure 12: Contour plot of velocity magnitude and direction of peak flow speed during deployment.

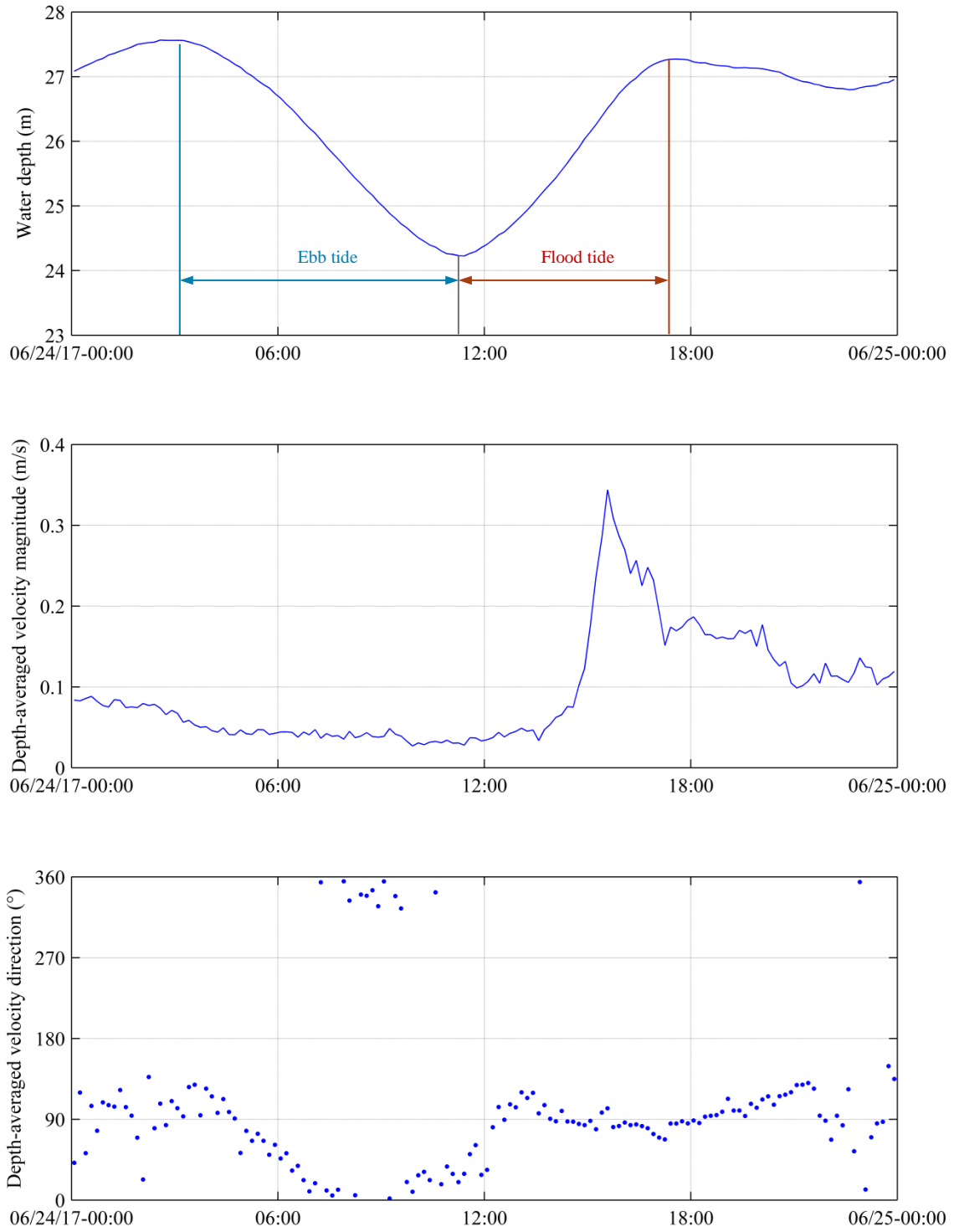


Figure 13: Water depth (top), depth-averaged velocity magnitude (middle) and depth-average flow direction (bottom) for tide of peak flow speed during deployment

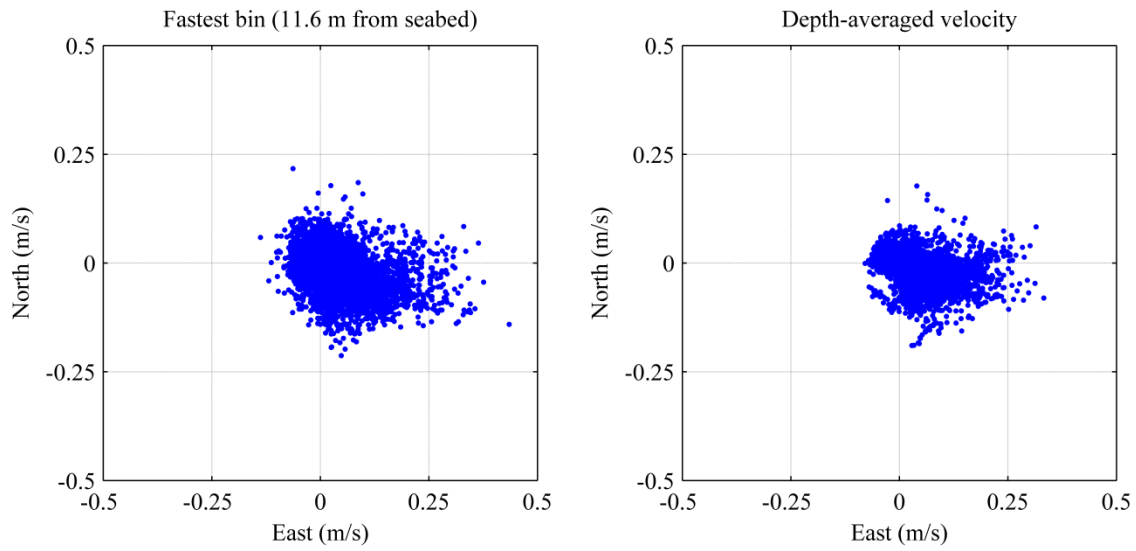


Figure 14: Scatter plot of velocity using velocities from the depth of the fastest velocity recording (left) and depth-averaged velocities (right).

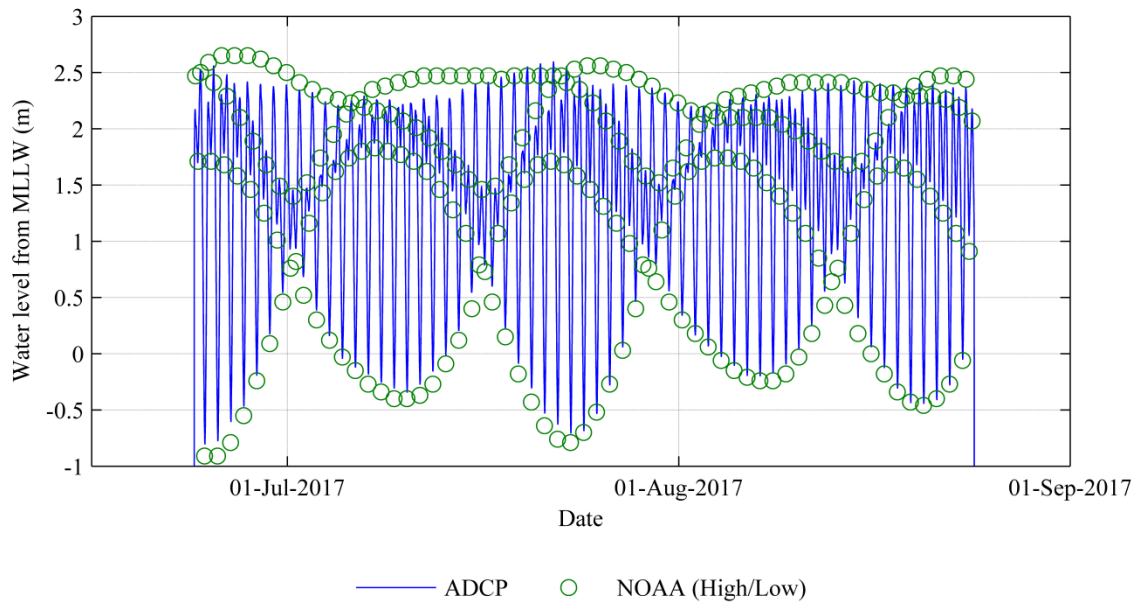


Figure 15: Water level time series from ADCP measurements and NOAA high/low tidal elevation prediction.

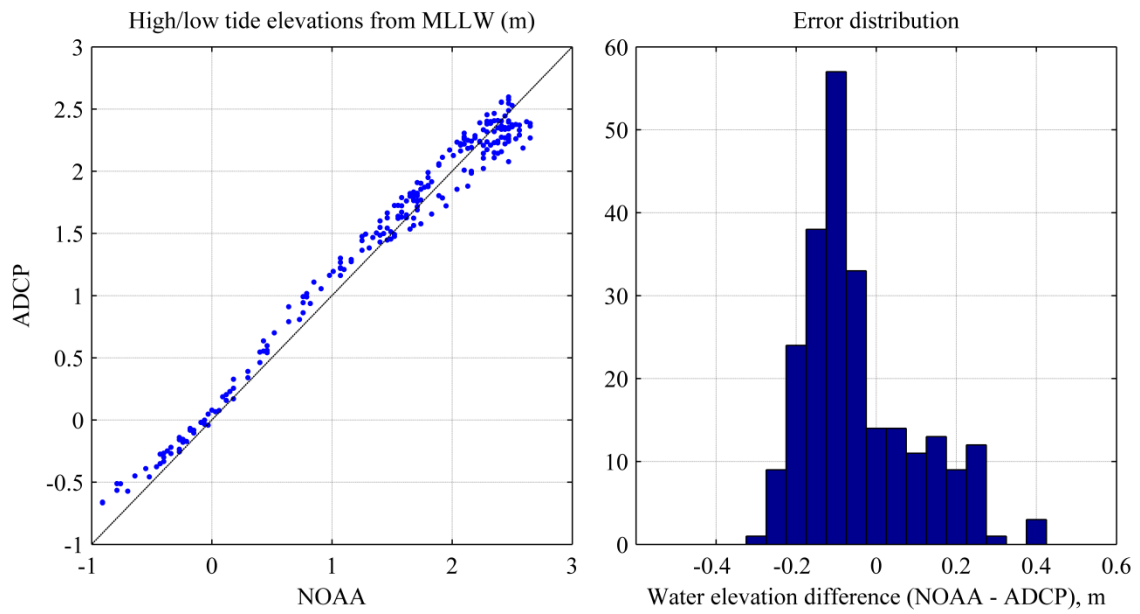


Figure 16: Comparison of NOAA tidal elevation prediction and ADCP measurements.

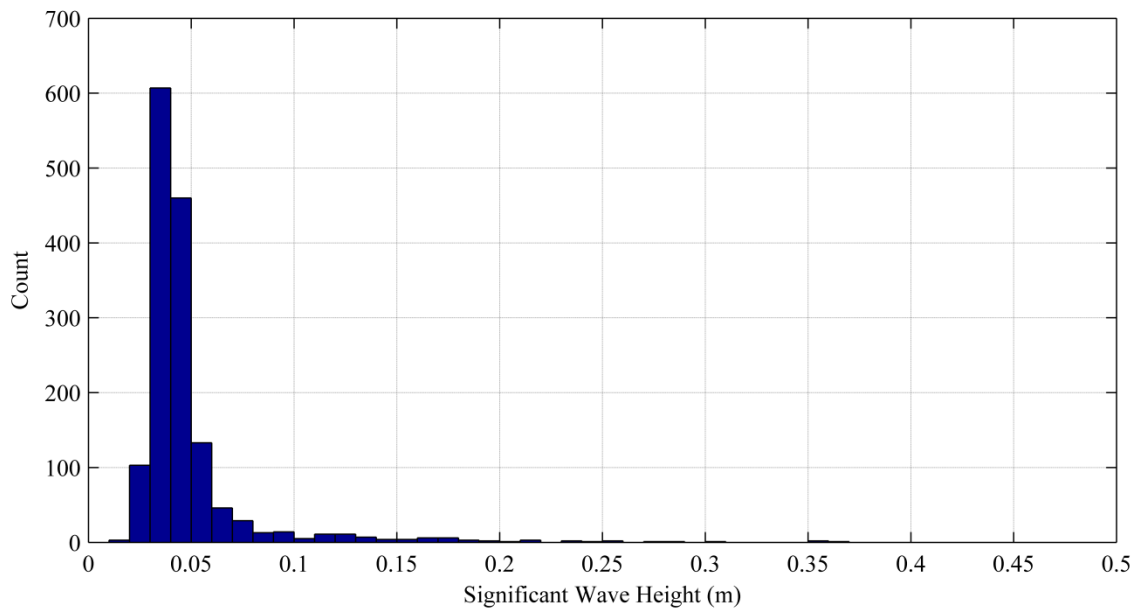


Figure 17: Distribution of significant wave height during deployment

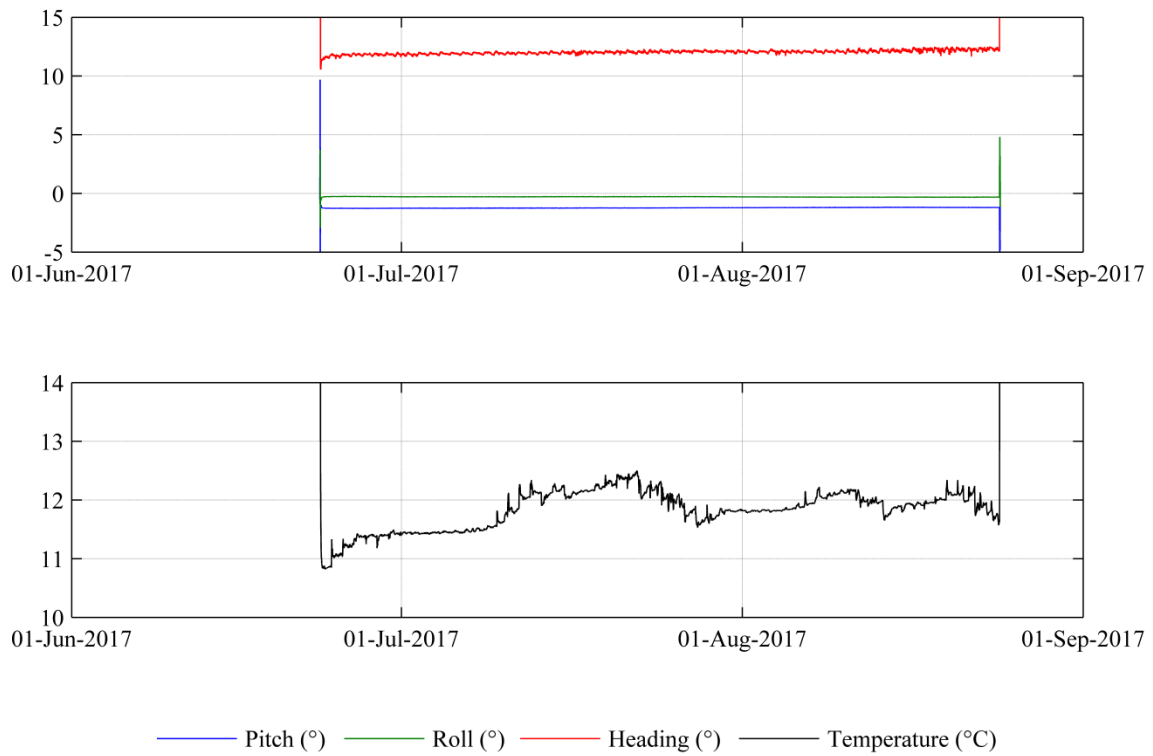


Figure 18: Ancillary data of instrument pitch, roll and heading (top) and water temperature (bottom) throughout the deployment.

5.0 References

- Brumley BH, KL Deines, RG Cabrera, and EA Terray. May 1993. *Broadband Acoustic Doppler Current Profiler*, US Patent 5, 208, 785.
- Gordon RL. 1989. Acoustic Measurement of River Discharge. *Journal of Hydraulic Engineering* (ASCE), 115(7):925-936.
- RDI. 1996. *Acoustic Doppler Current Profiler: Principles of Operation – A Practical Primer*, Teledyne RD Instruments, California, 2nd Edition.
- RDI. 1998. *ADCP Coordinate Transformation: Formulas and Calculation*. , Teledyne RD Instruments
- Schott F. 1987. Medium-range vertical acoustic Doppler current profiling from submerged buoys. *Deep Sea Research Part A - Oceanographic Research*, 33(10):1279-1292.

Appendix A
ADCP Operating Principle

Appendix A

ADCP Operating Principle

Use of acoustic Doppler current profilers to collect water velocity profiles has been widely documented in the technical literature since the 1980s (see Gordon, 1989; Schott, 1987; Brumley et al., 1993). ADCPs work by transmitting acoustic pulses from three or four diverging acoustic transducers (see Figure 19).

The transducers are typically spaced at equal azimuth intervals from one another at an angle of 20°-25° from vertical. After the pulse is emitted, the ADCP then listens to and processes returned echoes from successively farther away water volumes along the beams to determine how much the frequency has changed. The difference in frequency between transmitted and reflected sound is proportional to the relative velocity between the ADCP and the scatterers in the water based on the Doppler shift

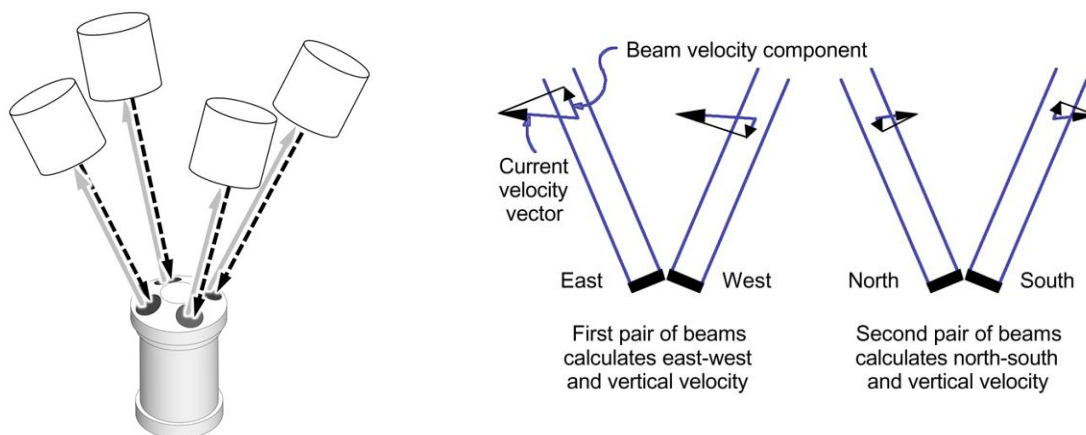


Figure 19: Schematic of RDI Workhorse Sentinel ADCP (left), showing the direction of the transmitted acoustic signal in grey, and the reflected signal in black. Beam velocity schematic (right) shows how a velocity vector is projected as a beam-wise component and a cross-beam component. Cardinal directions given in the right-side figure are for descriptive purposes only (RDI, 1996).

Defining the flow speed in the direction of the beam as positive velocity towards the instrument, the coordinate transformation from beam coordinates to instrument coordinates is given by Equation 1 to Equation 3. The angle of divergence of each acoustic beam from the instrument axis is defined as $\theta = 20^\circ$.

$$u_j = \frac{b_{1,j} - b_{2,j}}{2 \sin \theta} \quad \text{Equation 1}$$

$$v_j = \frac{b_{3,j} - b_{4,j}}{2 \sin \theta} \quad \text{Equation 2}$$

$$w_j = \frac{b_{1,j} + b_{2,j} + b_{3,j} + b_{4,j}}{4 \cos \theta} \quad \text{Equation 3}$$

A three-dimensional velocity is able to be calculated using the Doppler shift in three beams. Thus, with a four-beam instrument, the redundant beam allows the calculation of an error metric, defined by Equation 4.

$$e_{i,j} = \frac{b_{1,j} + b_{2,j} - b_{3,j} - b_{4,j}}{\sqrt{8} \sin \theta} \quad \text{Equation 4}$$

The velocity vector is transformed from the instrument coordinate system to earth coordinate system using Euler angle matrix transformation is given in Equation 5, for pitch, roll and yaw angles of ϕ , ϑ and ψ , respectively. Note that in the case of the upwards looking instrument, 180° must be added to the measured roll before applying this coordinate transform (RDI, 1998).

$$R = \begin{bmatrix} \cos \psi & \sin \psi & 0 \\ -\sin \psi & \cos \psi & 0 \\ 0 & 0 & 1 \end{bmatrix} \begin{bmatrix} 1 & 0 & 0 \\ 0 & \cos \phi & -\sin \phi \\ 0 & \sin \phi & \cos \phi \end{bmatrix} \begin{bmatrix} \cos \vartheta & 0 & \sin \vartheta \\ 0 & 1 & 0 \\ -\sin \vartheta & 0 & \cos \vartheta \end{bmatrix} \quad \text{Equation 5}$$

The relationship between the velocity components in the instrument coordinate system and those in the earth coordinate system is then given in Equation 6.

$$\begin{bmatrix} E \\ N \\ Up \end{bmatrix} = R \begin{bmatrix} u \\ v \\ w \end{bmatrix} \quad \text{Equation 6}$$

Appendix B

Deployment configuration file

Appendix B

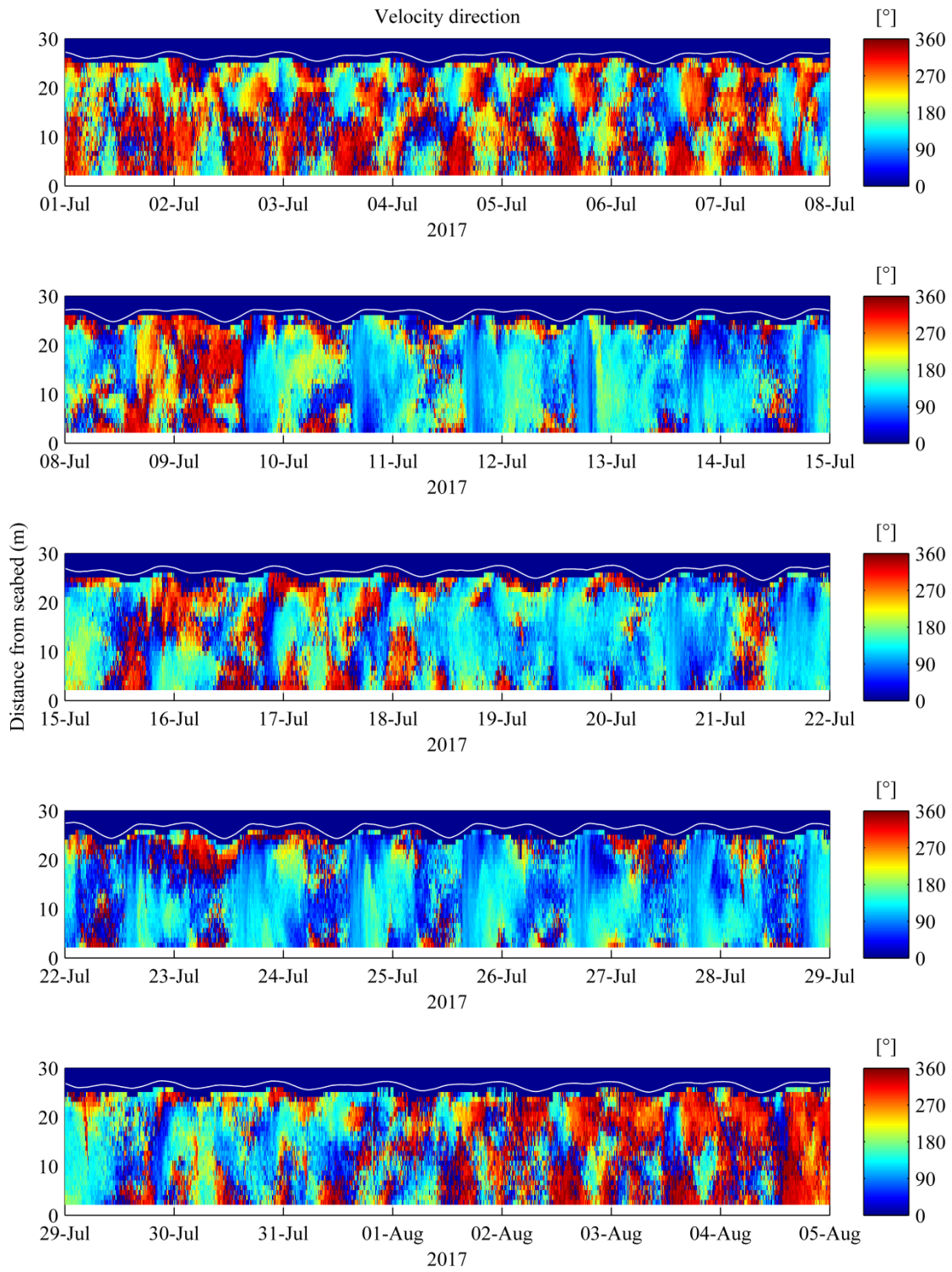
Deployment configuration file

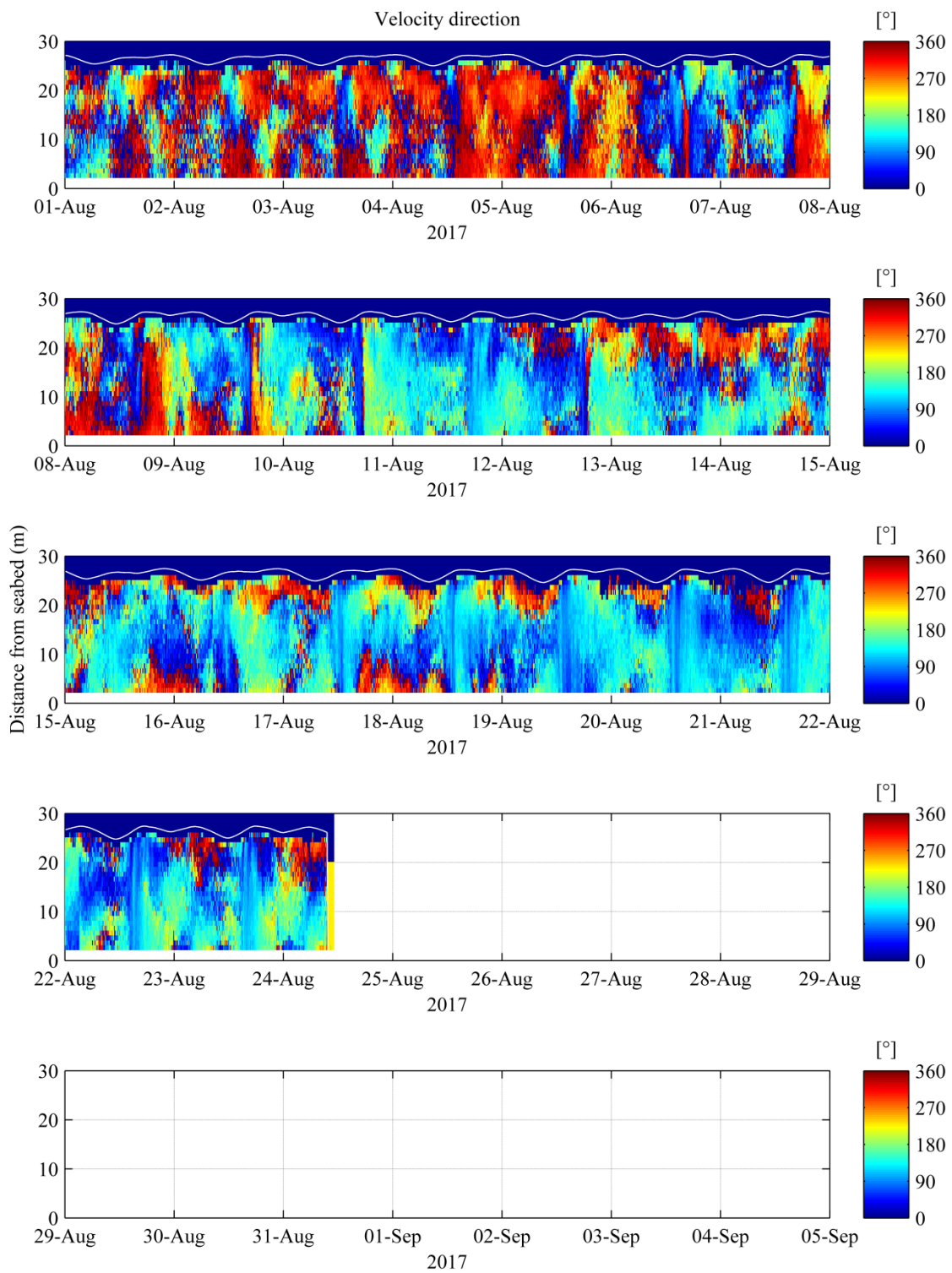
Deployment_Config_BEAM_230617.txt

CR1
CF11101
EA0
EB1605
ED300
ES35
EX00000
EZ1111101
WA255
WB0
WD111100000
WF88
WN35
WP24
WS100
WV175
HD111000000
HB5
HP1200
HR01:00:00.00
HT00:00:00.50
TE00:10:00.00
TP00:05.00
CK
CS

Appendix C

Contour plots of velocity direction







Pacific Northwest
NATIONAL LABORATORY

*Proudly Operated by **Battelle** Since 1965*

902 Battelle Boulevard
P.O. Box 999
Richland, WA 99352
1-888-375-PNNL (7665)

U.S. DEPARTMENT OF
ENERGY

www.pnnl.gov